



Published in final edited form as:

ACS Chem Biol. 2010 February 19; 5(2): 183–194. doi:10.1021/cb900218c.

## Selective inhibition of DNA replicase assembly by a non-natural nucleotide: Exploiting the structural diversity of ATP-binding sites

Kevin Eng<sup>a</sup>, Sarah K Scouten-Ponticelli<sup>b</sup>, Mark Sutton<sup>b</sup>, and Anthony Berdis<sup>a,#</sup>

<sup>a</sup>Department of Pharmacology, Case Western Reserve University, Cleveland OH 44106

<sup>b</sup>Department of Biochemistry, University of Buffalo, State University of New York, Buffalo NY, 14214

### Abstract

DNA synthesis is catalyzed by an ensemble of proteins designated the replicase. The efficient assembly of this multi-protein complex is essential for the continuity of DNA replication and is mediated by clamp-loading accessory proteins that use ATP binding and hydrolysis to coordinate these events. As a consequence, the ability to selectively inhibit the activity of these accessory proteins provides a rational approach to regulate DNA synthesis. Toward this goal, we tested the ability of several non-natural nucleotides to inhibit ATP-dependent enzymes associated with DNA replicase assembly. Kinetic and biophysical studies identified 5-nitro-indolyl-2'-deoxyribose-5'-triphosphate as a unique non-natural nucleotide capable of selectively inhibiting the bacteriophage T4 clamp loader versus the homologous enzyme from *Escherichia coli*. Modeling studies highlight the structural diversity between the ATP-binding site of each enzyme and provide a mechanism accounting for the differences in potencies for various substituted indolyl-2'-deoxyribose-5'-triphosphates. An *in vivo* assay measuring plaque formation demonstrates the efficacy and selectivity of 5-nitro-indolyl-2'-deoxyribose as a cytostatic agent against T4 bacteriophage while leaving viability of the *E. coli* host unaffected. This strategy provides a novel approach to develop agents that selectively inhibit ATP-dependent enzymes that are required for efficient DNA replication.

### Keywords

Non-natural nucleotides; processivity factors; ATPase activity; DNA replication; inhibitors

---

DNA replication is essential for the proliferation and survival of all forms of life ranging from simple viruses and bacteria to more complex organisms including humans. The effect of uncontrolled DNA synthesis is often highlighted by various pathological states caused by dysfunctional and/or unregulated replication activity. Diseases such as cancer, autoimmune disorders, and viral infections require abnormally high levels of DNA synthesis. As a

---

<sup>#</sup>Corresponding Author Information: Telephone (216)-368-4723, Fax (216)-368-1030, ajb15@case.edu.

### Supporting Information Available

The supporting information file contains the following: (1) a plot comparing the  $K_i$  value of non-natural nucleotides for gp44/62 versus nucleotide shape and size (defined as  $\text{\AA}^3$ ); (2) a comparison of the primary amino acid sequence encompassing the ATP binding regions of clamp loaders from T4 bacteriophage (gp44/62), *E. coli* ( $\gamma$ -complex), and *S. cerevisiae* (RFC); (3) a comparison of the cytotoxic effects of d5-NI, chloramphenicol, and DMSO via a colony forming assay using JA300 *E. coli* cells; (4) different kinetic simulations illustrating how the sensitivity factor for d5-NITP is influenced as a function of various experimental conditions (i.e., changes in substrate concentration, changes in enzyme concentration, etc.); and (5) an illustration highlighting the differences between replication in *E. coli* versus bacteriophage T4.

consequence, these pathological states are treated with compounds that inhibit DNA synthesis. DNA damaging agents and chain-terminating nucleosides hinder DNA replication by chemically transforming nucleic acid into an ineffective substrate for elongation (1). Unfortunately, these agents often cause severe side effects induced by the non-selective killing of pathogenic and healthy cells (2). In addition, these agents can accelerate disease development by altering the integrity and stability of genomic material (3). For example, anti-viral nucleosides can cause symptoms mimicking diabetes mellitus (4) while DNA damaging agents are linked with the development of therapy-related cancers (5).

To avoid these complications, other molecular targets involved in DNA synthesis must be evaluated as potential points for therapeutic intervention. Indeed, efficient DNA replication is dependent upon a confederation of proteins (6) that must function in a collaborative effort. Several of these proteins, including DNA helicases and "clamp-loading" accessory proteins, require ATP binding and hydrolysis to function properly (7). Clamp loaders are an attractive target as they function to increase the efficiency of DNA synthesis by placing accessory proteins, referred to as "sliding clamps", onto nucleic acid in an ATP-dependent manner. Sliding clamps increase the processivity of DNA polymerases involved in chromosomal replication, and disrupting the interactions between a DNA polymerase and its processivity factor dramatically reduces the overall efficiency of DNA synthesis (8). Since replicative accessory proteins are species-specific, inhibiting the function of a pathogenic protein without affecting the activity of the host protein could be developed into a selective therapeutic agent to inhibit cellular proliferation.

However, this is not an easy task since clamp loaders from viruses, bacteria, and eukaryotes all rely on the binding and hydrolysis of ATP for their biological function. As such, the commonality in primary amino acid sequence for the ATP binding site suggests a low probability of identifying a unique molecule that inhibits a clamp loader from one species while leaving another unaffected. In spite of these obstacles, this report describes the ability of various non-natural nucleotides (Figure 1) to disrupt processive DNA synthesis by inhibiting the activity of ATP-dependent accessory proteins. Kinetic, biophysical, and *in vivo* data reveal a specific non-natural nucleotide, 5-nitro-indolyl-2'-deoxyribose-5'-triphosphate (d5-NITP) 1, that selectively inhibits the bacteriophage T4 clamp loader versus the functionally homologous clamp loader from *Escherichia coli*. This represents a novel strategy to develop therapeutic agents against hyperproliferative diseases such as viral infections and cancer by selectively inhibiting ATP-dependent enzymes involved in DNA replication and recombination.

## RESULTS AND DISCUSSION

### d5-NITP is a Potent Inhibitor of the Bacteriophage T4 Clamp Loader

d5-NITP is a non-natural nucleotide that mimics the size and shape of (d)ATP (Figure 1A) and is used as an effective surrogate for dATP by various DNA polymerases during the misreplication of damaged DNA (9). These features prompted us to evaluate if d5-NITP

<sup>1</sup>Abbreviations: d4-NITP, 4-nitro-indolyl-2'-deoxyriboside triphosphate; d5-NITP, 5-nitro-indolyl-2'-deoxyriboside triphosphate; r5-NITP, 5-nitro-indolyl-2'-ribose triphosphate; d5-NI, 5-nitro-indolyl-2'-deoxyriboside; d6-NITP, 6-nitro-indolyl-2'-deoxyriboside triphosphate; d5-EtITP, 5-ethyl-indolyl-2'-deoxyriboside triphosphate; d5-EyITP, 5-ethylene-indolyl-2'-deoxyriboside triphosphate; d5-EyInd, 5-ethylene-indolyl-2'-deoxyriboside; d5-FITP, 5-fluoro-indolyl-2'-deoxyriboside triphosphate; d5-FI, 5-fluoro-indolyl-2'-deoxyriboside; dITP, indolyl-2'-deoxyriboside triphosphate; Ind, indolyl-2'-deoxyriboside; d5-CHITP, 5-cyclohexyl-indolyl-2'-deoxyriboside triphosphate; d5-AITP, 5-amino-indolyl-2'-deoxyriboside triphosphate; d5-CEITP, 5-cyclohexene-indolyl-2'-deoxyriboside triphosphate; d5-CITP, 5-carboxylate-indolyl-2'-deoxyriboside triphosphate; d5-PhITP, 5-phenyl-indolyl-2'-deoxyriboside triphosphate; AMP-PNP, 5'-adenylyl-beta, gamma-imidodiphosphate; gp44/62, bacteriophage T4 sliding clamp loader; gp45, bacteriophage T4 sliding clamp; gp43 exo<sup>-</sup>, exonuclease-deficient mutant of bacteriophage T4 DNA polymerase;  $\gamma$  complex, *E. coli* sliding clamp loader;  $\beta$  clamp, *E. coli* sliding clamp.

could also act as a substrate for the ATP-dependent bacteriophage T4 clamp loader, gp44/62. Despite structural and functional similarities to dATP, d5-NITP is not hydrolyzed by gp44/62 (Figure 2A). The inability to hydrolyze d5-NITP is not caused by the absence of the 2'-hydroxyl moiety since gp44/62 is also incapable of hydrolyzing r5-NITP, the ribose form of the non-natural nucleotide (Fig 2A). This contrasts data obtained with natural nucleotides in which gp44/62 hydrolyzes dATP just as efficiently as ATP (Fig 2A).

The lack of hydrolysis could simply reflect an inability to bind the non-natural nucleotide. This possibility was tested by monitoring the dose-dependency of d5-NITP toward inhibiting the ATPase activity of gp44/62. Figure 2B shows that d5-NITP inhibits gp44/62 with a  $K_i$  value of  $4.8 \pm 0.5 \mu\text{M}$ . A similar  $K_i$  of  $10.8 \pm 0.7 \mu\text{M}$  is obtained using r5-NITP (Figure 2B), indicating that the bacteriophage clamp loader is promiscuous in its ability to bind either ribose or deoxyribose nucleotides (10). The calculated Hill coefficient for both non-natural nucleotides is  $\sim 1$ , indicating a lack of positive or negative cooperativity between the four ATP binding sites of gp44/62.

The mode of inhibition by d5-NITP was determined by measuring ATP hydrolysis at several different fixed concentrations of d5-NITP while varying the concentration of ATP. The double reciprocal plot yields a series of lines intersecting on the y-axis and are diagnostic for reversible, competitive inhibition (Figure 2C) (11). The measured  $K_i$  of  $5.7 \pm 1.1 \mu\text{M}$  is identical, within error, to the value of  $4.8 \mu\text{M}$  measured using Dixon plot analysis. It is striking that the  $K_i$  for d5-NITP is  $\sim 5$ -fold lower than the inhibition constant of  $29 \mu\text{M}$  for ATP $\gamma$ S (Table 1) and  $\sim 300$  fold lower than the value of  $1,200 \mu\text{M}$  measured for AMP-PNP (12). The lower inhibition constant for d5-NITP compared to these other competitive inhibitors indicates superior binding affinity that is influenced by the unique chemical features present on the 5-nitro-indolyl moiety. However, the triphosphate group is essential for binding as 5-nitro-indolyl 2'-deoxynucleoside (d5-NI) does not inhibit gp44/62 at concentrations greater than  $200 \mu\text{M}$ .

### **d5-NITP inhibits DNA synthesis by blocking replicase assembly**

gp44/62 catalyzes formation of the replicase, a multi-protein complex that performs highly processive DNA synthesis. During this process, gp44/62 binds and hydrolyzes (d)ATP to first load the processivity factor, gp45, onto DNA and then coordinates proper interactions of gp45 with the DNA polymerase (gp43) in an ATP-independent manner (13). Although gp44/62 does not hydrolyze d5-NITP, we tested if replicase formation can occur solely through the binding of the non-natural nucleotide using the strand displacement polymerization assay (14) (Figure 3A). This assay distinguishes between processive DNA synthesis catalyzed by replicase complex (synthesis beyond a forked strand) from the activity of DNA polymerase that does not perform strand displacement synthesis. As illustrated in Figure 3B, longer replication products are generated by the replicase compared to DNA polymerase alone (compare lane 4 with lane 2). The inclusion of  $100 \mu\text{M}$  d5-NITP inhibits formation of the replicase complex as shorter replication products are produced (Figure 3B, lane 5) compared to when d5-NITP is omitted (Figure 3B, lane 4). The reduction in processive DNA synthesis does not reflect direct inhibition of polymerase activity by d5-NITP since identical amounts of products are generated by the polymerase in the absence or presence of d5-NITP (Figure 3C). The lack of an effect on polymerase activity is consistent with reports indicating that d5-NITP is poorly incorporated opposite any of the four natural templating nucleobases (15,16).

The inhibitory effect by d5-NITP on gp44/62 was further investigated using a FRET quenching assay developed by Benkovic and co-workers (17) that monitors the ability of gp44/62 to open the closed ring of the homotrimeric gp45 labeled with fluorescent probes. When CPM-labeled gp45 is mixed with gp44/62 and  $1 \text{ mM}$  ATP, a rapid change in

fluorescence with an amplitude of  $0.2199 \pm 0.0004$  units is obtained (Figure 3D) and confirms that clamp opening occurs upon ATP binding and hydrolysis. However, a significantly smaller change in fluorescence (amplitude =  $0.044 \pm 0.002$ ) is detected when ATP is replaced with 1 mM d5-NITP (Figure 3D), indicating that clamp opening does not occur upon binding of the non-natural nucleotide. These results collectively indicate that d5-NITP inhibits replicase assembly and subsequent processive DNA synthesis by hindering the ability of gp44/62 to open the closed gp45 trimer.

### Structure-activity relationships for nucleotide binding

d5-NITP represents the most potent inhibitor of gp44/62 identified to date as it binds 5- and 300-fold more tightly than other competitive inhibitors such as ATP $\gamma$ S and AMP-PNP, respectively. A structure-activity relationship explaining the unprecedented potency of d5-NITP was developed by testing the ability of the other non-natural nucleotides (Figure 1B) to inhibit gp44/62. The data summarized in Table 1 indicate that the active site of gp44/62 displays an unexpected plasticity in its ability to bind a variety of non-natural nucleotides of diverse size and shape. Although these analogs bind with differing affinities, a direct correlation between binding affinity and nucleobase size is not evident (Supplemental Information 1). In fact, d5-NITP binds with a significantly higher affinity compared to analogs such as ATP $\gamma$ S and AMP-PNP that are similar in shape and size. In addition, the majority of small non-natural nucleotides such as dITP, d5-AITP, and d5-FITP bind poorly as their  $K_i$  values are greater than 200  $\mu$ M. One notable exception is d5-EtITP as it inhibits gp44/62 with a  $K_i$  value of 80  $\mu$ M. Surprisingly, the closely related analog, d5-EyITP, binds far worse with a  $K_i$  greater than 200  $\mu$ M. The unexpected difference in potency between the two analogs may be caused by entropic factors as the more flexible ethyl moiety could occupy lower free energy states associated with ground state binding compared to the conformationally restricted ethylene moiety.<sup>2</sup> Indeed, entropic effects appear to play important roles in binding as bulky, hydrophobic analogs such as d5-CHITP and d5-PhITP bind to gp44/62 with low  $K_i$  values of  $\sim 40$   $\mu$ M. The  $K_i$  values of these analogs are lower than analogs such as dITP and d5-AITP that more closely resemble ATP, and again reiterate that nucleobase size or shape does not directly correlate with binding affinity.

In addition, a strong correlation between binding affinity and overall  $\pi$ -electron surface area is not apparent since the  $K_i$  value for the electron rich d5-PhITP ( $K_i = 42$   $\mu$ M) is identical to that for d5-CHITP ( $K_i = 42$   $\mu$ M) which lacks significant  $\pi$ -electron density at the 5-position. It is quite surprising that the hydrophilic analog, d5-CITP, binds to gp44/62 with a relatively low  $K_i$  of 37  $\mu$ M. This provides an interesting paradox as the small hydrophilic nucleotide, d5-CITP, binds with nearly the same affinity as large, hydrophobic analogs such as d5-CHITP and d5-PhITP. This dichotomy becomes even more intriguing when one considers that d5-NITP, an analog possessing both hydrophobic and hydrophilic character, binds 5-fold more tightly than any of these analogs.

### Exploring the active site of gp44/62

Predictive *in silico* models of the active site of gp44/62 bound with ATP (Figure 4A) or with d5-NITP (Figure 4B) were generated to provide more insight into the mechanism of nucleotide binding. In the absence of a structure for gp44/62, the PHYRE (18) server was used to create a threaded model based on the structure of *P. furiosus* RFC (1IQP) with a high degree of confidence ( $E$  value of  $2.5 \times 10^{-27}$ ). In this model, gp44/62 binds ATP through interactions with each individual component of the nucleoside triphosphate. The

<sup>2</sup>An alternative model proposed by an anonymous reviewer of this manuscript is that the differences in binding affinities between d5-EtITP and d5-EyITP reflect forced desolvation of positively and/or negatively charged amino acids within the active site of gp44/62. This could also explain the low  $K_i$  value measured for d5-NITP.

triphosphate moiety interacts with a positively charged arginine (Arg205) as well as G55, K56, and T57 that compose part of the Walker A motif. The hydroxyl group on the ribose moiety interacts with Arg16 through hydrogen bonding interactions while contacts with the adenine ring are stabilized through  $\pi$ - $\pi$  stacking interactions with Phe204 and hydrogen-bonding interactions with amide bonds on the adjacent helix.

The model of gp44/62 bound with d5-NITP shows many of the same interactions. Two noticeable differences, however, include more favorable stacking interactions between the indolyl ring and Phe204 as well as potential electrostatic interactions between the nitro group and Arg175. This model shows strong alignment between the two oxygens on the nitro moiety with the guanidinium nitrogens of Arg175 that is not present in the model of gp44/62 bound with ATP. As such, the orientation and close proximity ( $<4\text{\AA}$ ) between these complementary functional groups could account for the higher affinity of d5-NITP compared to ATP.

To investigate this mechanism, inhibition constants for d5-NITP were measured using two active site mutants, R175L and R175K (Table 2). The binding affinity for d5-NITP decreases  $\sim 3$ -fold upon the conservative substitution of arginine with lysine. This small decrease is consistent with a minimal loss of electrostatic interactions between the oxygens of the nitro group and the guanidinium nitrogen. Surprisingly, the  $K_i$  of  $16\ \mu\text{M}$  for the R175L mutant is identical to  $14\ \mu\text{M}$  measured with the R175K mutant. At face value, this result is unexpected since replacing the positively charged arginine with the hydrophobic leucine should abrogate electrostatic interactions and thus weaken binding affinity by at least 10-fold. However, hydrophobic interactions between the nitro and leucine most likely compensate for the loss of the electrostatic interaction. Indeed, the identity in  $K_i$  values for d5-NITP with the R175K and R175L mutants likely reflects its bipolar character as d5-NITP possesses both hydrophilic and hydrophobic properties. This possibility was investigated by measuring the inhibition constant for d5-CITP with these mutants. The  $K_i$  of  $41\ \mu\text{M}$  with the R175K mutant is very similar to the  $K_i$  of  $37\ \mu\text{M}$  with wild-type gp44/62. This minimal change is expected since the carboxyl moiety can form favorable electrostatic contacts with either arginine or lysine. However, a more dramatic effect is observed with the R175L mutant as reflected by the large  $K_i$  of  $>200\ \mu\text{M}$ , indicating that replacement of a positively charged amino acid with the hydrophobic leucine adversely influences the binding of the negatively charged d5-CITP.

Additional evidence for the role of Arg175 in binding non-natural nucleotides comes from comparing the  $K_i$  values for hydrophobic analogs such as d5-EtITP and d5-EyITP (Table 2). These analogs bind poorly to wild-type and R175K mutant. However, their  $K_i$  values are  $\sim 10$ -fold lower in the R175L mutant compared to wild type enzyme. This increase in binding affinity is consistent with a model invoking entropic stabilization of the hydrophobic nucleobase within a hydrophobic active site upon replacement of arginine with leucine. By inference, these data suggest that the high binding affinity of d5-NITP is caused by the schizophrenic nature of the nitro moiety which can interact with positively charged amino acids through enthalpic effects and with hydrophobic amino acids through entropic/desolvation effects.

At the molecular level, the nitro group appears to behave as a promiscuous pharmacophore as it can blend into different protein environments with diverse functional groups such as positively charged and hydrophobic amino acids. In this case, the electron withdrawing potential and zwitterionic character of  $-\text{NO}_2$  allows it to participate in non-covalent, electrostatic interactions while its double-bond character provides potential interactions through  $\pi$ -cation and  $\pi$ - $\pi$  stacking arrangements. Finally, the surprisingly low solvation energy of the nitro moiety allows it to interact with molecular targets through entropic

effects. These collective properties provide d5-NITP with its superior inhibitory effects against ATP-dependent clamp loaders, especially compared with other competitive inhibitors such as ATP $\gamma$ S and AMP-PCP that accurately mimic ATP. Since the triphosphate moiety of d5-NITP is unmodified, inhibition displayed by this non-natural nucleotide likely occurs via non-productive binding that prevents conformational changes in gp44/62 required for proper interactions with gp45. We argue that interactions between d5-NITP and specific amino acids such as Arg175 and Phe204 within the ATP-binding site are responsible for non-productive binding as these interactions do not exist when ATP is bound to gp44/62.

To investigate this further possibility, we measured the  $K_i$  values for d4-NITP and d6-NITP to evaluate if the position of the nitro pharmacophore impacts nucleotide binding. With wild type gp44/62, the  $K_i$  of 34  $\mu$ M for d4-NITP is ~6-fold higher than that for d5-NITP (5.7  $\mu$ M) and suggests that placement of the nitro group at the 4-position prohibits favorable contacts with Arg175 (Table 1). Consistent with this argument, the  $K_i$  value for d4-NITP is unaltered when Arg175 is replaced with either lysine or leucine (Table 2). In contrast, the  $K_i$  for d6-NITP (5.1  $\mu$ M) is identical to that for d5-NITP (4.8  $\mu$ M) and suggests that the binding mode for d6-NITP and d5-NITP are identical (Table 1). However, the model in Figure 4B argues otherwise as Arg175 does not directly interact with the pharmacophore at the 6-position. Instead, the high binding affinity for d6-NITP likely results from favorable electrostatic interactions with Arg16, another positively charged amino acid in close proximity. Collectively, these data indicate that the position of the nitro pharmacophore influences binding affinity through discrete molecular contacts with active site amino acids.

### d5-NITP is a selective inhibitor of gp44/62

Clamp loaders across all species serve identical functions by using ATP to assemble their respective DNA replicase complexes (19). In fact, the clamp loaders from bacteriophage T4, *E. coli*, and eukaryotes all display significant similarity (~56%) and identity (~33%) in regions that interact with ATP (Supplemental Information 2). The similarities in function and active site composition predict that all clamp loaders should display an identical structure-activity relationship for the non-natural nucleotides used in this study. This hypothesis is inaccurate as the  $K_i$  values for non-natural nucleotides differ significantly between gp44/62 and the related *E. coli*  $\gamma$ -complex (Table 1). In fact, gp44/62 binds these analogs with affinities ranging from 5  $\mu$ M to greater than 200  $\mu$ M while the  $\gamma$ -complex binds the same analogs with an average affinity of ~20  $\mu$ M. Compared to gp44/62, the  $\gamma$ -complex binds the majority of analogs with higher affinity. In fact, d5-NITP is the only nucleotide analog that binds more tightly to gp44/62 than to the  $\gamma$ -complex. The difference in binding affinity provides a selectivity factor of 4.5 for the phage clamp loader whereas most other analogs display selectivity factors of <1 (Table 1).

The selectivity of d5-NITP was investigated comparing *in silico* models of the active site of the  $\gamma$ -complex (1NJF) bound with ATP (Figure 4C) or d5-NITP (Figure 4D) with corresponding models of gp44/62 (Figure 4A and 4B). Visual inspection reveals some obvious similarities between the two clamp loaders. The triphosphate moieties of ATP and d5-NITP interact with amino acids within the Walker A motif (G57, K58, and T59) as well as Arg63 in the *E. coli*  $\gamma$ -complex. A major difference between the two clamp loaders, however, is the absence of an aromatic amino acid in the active site of the  $\gamma$ -complex that can interact with adenine or the indole of d5-NITP. In addition, the  $\gamma$ -complex lacks a positively charged amino acid analogous to Arg175 in gp44/62 that could interact with the nitro pharmacophore. In fact, the active site of the  $\gamma$ -complex (Figure 4C) resembles a simple hydrophobic pocket lined with small, aliphatic amino acids including P12, V18, and V19. This hydrophobic environment could explain why most hydrophobic non-natural nucleotides bind with similar affinities (~20  $\mu$ M) that are relatively independent of shape/size,  $\pi$ -electron surface area, and dipole moment.

## Testing the *in vivo* selectivity of non-natural nucleosides

We hypothesize that the differences in  $K_i$  values for d5-NITP between clamp loaders could be exploited to inhibit phage replication while leaving DNA synthesis in the *E. coli* host unperturbed. This system provides a simple and convenient model to test non-natural nucleos(t)ides as potential agents that selectively inhibit pathogenic DNA synthesis in a host. This was investigated using a plaque-forming assay to quantify the ability of non-natural nucleosides to inhibit phage infection in an *E. coli* host (20). Data provided in Figure 5A shows that *E. coli* preincubated with 100  $\mu\text{g/mL}$  d5-NI have ~40% fewer plaques compared to untreated *E. coli*. The protective effect is dose-dependent as treatment with 25  $\mu\text{g/mL}$  d5-NI provides ~2.5-fold less protection than 50  $\mu\text{g/mL}$  (Figure 5B). It should be emphasized that the nitro group acts as the primary pharmacophore since other non-natural nucleosides generate significantly less protective effects. This is evident as treatment with 150  $\mu\text{g/mL}$  5-ethylene-indolyl-2'-deoxyribose (d5-Ey) only inhibits 15% of plaque formation while other analogs such as 5-fluoro-indolyl-2'-deoxyribose (d5-FI) do not inhibit plaque formation at concentrations of 100  $\mu\text{g/mL}$  (Figure 5C).

The reduction in phage infectivity by d5-NI does not appear to be caused by an indirect mechanism such as reducing the viability of *E. coli*. This conclusion is based upon several independent pieces of evidence. First, d5-NI does not produce a significant bactericidal or bacteriostatic effect on *E. coli* in suspension (Figure 5D) or when plated on LB/agar for extended periods of time (Supplemental Information 3). Secondly, the inclusion of a bacteriostatic agent such as the antibiotic chloramphenicol does not cause an appreciable decrease in phage infectivity (Figure 5C). Finally, the inability of other non-natural nucleoside analogs such as d5-5Ey and d5-FI to inhibit plaque formation correlates well with the poor potency of the corresponding nucleoside triphosphate to inhibit gp44/62. In fact, the protective effects of 100  $\mu\text{g/mL}$  of d5-NI against phage infection correlates with the *in vitro* inhibitory effects of d5-NITP against the bacteriophage clamp loader. Indeed, simple calculations predict that complete conversion of 100  $\mu\text{g/mL}$  of d5-NI to the corresponding triphosphate would generate a maximum intracellular concentration of 200  $\mu\text{M}$  d5-NITP. This concentration would be sufficient to inhibit greater than 98% of gp44/62 activity *in vivo* as it is >40 times the  $K_i$  value of 4.7  $\mu\text{M}$  measured for d5-NITP. We acknowledge that complete conversion of d5-NI to d5-NITP is unlikely. However, even a low conversion efficiency of 10% would result in an intracellular concentration of 20  $\mu\text{M}$  d5-NITP. This concentration would still produce an appreciable inhibitory effect on the bacteriophage clamp loader while having a minimal effect on the *E. coli* clamp loader that possesses a higher  $K_i$  value for d5-NITP.

To investigate if the effects of d5-NI are dependent upon nucleoside phosphorylation, we measured the ability of this non-natural nucleoside to inhibit phage infection in an *E. coli* strain lacking deoxythymidine kinase activity (*E. coli* strain KY895). Reducing nucleoside phosphorylation activity should result in a lower intracellular concentration of d5-NITP which would reduce the inhibitory effects in phage infectivity. This would be manifest in an increase in plaque formation. Indeed, the protective effects of d5-NI appear to be dependent upon its conversion to d5-NITP as the data provided in Figure 5E show that the effects of d5-NI are significantly reduced in a deoxythymidine kinase deficient (*tdk-1*) *E. coli* strain (KY895) compared to wild-type *E. coli* (JA300). Experiments to accurately quantify the concentration of non-natural nucleotides in these *E. coli* strains are currently being performed to validate this proposed mechanism. Regardless, the data presented here suggest the inhibitory effects of d5-NI on phage infectivity are linked with the enzymatic formation of the nucleoside triphosphate.

Collectively, the *in vitro* and *in vivo* data presented here demonstrate that replicative accessory proteins are bona fide targets for therapeutic intervention against pathological

disorders caused by uncontrollable DNA synthesis. Although inhibiting DNA polymerase activity is the most logical target for therapeutic intervention, agents targeting this activity can cause toxic side effects by non-selectively inhibiting DNA synthesis in diseased *and* healthy cells. Using the simple bacteriophage T4 replication system as a tool, this report illustrates a way to circumvent this complication by selectively inhibiting DNA synthesis by targeting the activity of an essential replicative accessory protein. In this respect, the ability of the non-natural nucleoside, d5-NI, to differentially inhibit bacteriophage infectivity without affecting *E. coli* proliferation likely reflects the ability of the corresponding nucleotide to inhibit ATP-dependent processes involved in assembly of protein complexes at the DNA replication fork of the bacteriophage. From a pharmacological perspective, this preferential inhibition can be rationalized by simply evaluating the selectivity factor for d5-NITP, defined as the ratio of its  $K_i$  value for  $\gamma$ -complex versus gp44/62 ( $K_{i\text{ host}}/K_{i\text{ pathogen}}$ ). In general, high values of greater than 100 are desired as they predict exclusive inhibition of the target enzyme without influencing the activity of enzymes present in the host. As such, it is quite surprising that d5-NI displays any *in vivo* selectivity since the calculated *in vitro* selectivity factor for d5-NITP is only 4.5. This low value suggests that d5-NITP should elicit an appreciable cytostatic effect against *E. coli* by inhibiting bacterial DNA synthesis. However, this dichotomy can be rectified by taking into account a limitation of "selectivity" which assumes that the  $K_m$  value for the substrate will be identical amongst all potential targets. Indeed, selectivity factors can greatly underestimate the therapeutic potential of a compound if  $K_m$  values for the substrate differ by only 5-fold amongst various enzyme targets. As such, the therapeutic potential of an inhibitor must take into account the relationship between the  $K_i$  for the inhibitor with respect to the  $K_m$  for the substrate. This relationship, calculated as the ratio of  $[(K_m/K_i)_{\text{pathogen}}]/[(K_m/K_i)_{\text{host}}]$ , defines the *sensitivity factor* for an inhibitor. Using the parameters listed in Table 1, the sensitivity factor for d5-NITP against gp44/62 is 20, and this higher value could explain the cytostatic effects of d5-NI against phage proliferation *in vivo*. Kinetic simulations of this model (Supplemental Information 4) indicate that differences in the  $K_m$  for ATP will cause a competitive inhibitor such as d5-NITP to have a more pronounced inhibitory effect on the ATPase activity of the bacteriophage clamp loader compared to the  $\gamma$ -complex.

Another possibility is that fundamental differences in the biology of DNA replication between *E. coli* and the phage invader may contribute to the inhibitory effects of d5-NITP (Supplemental Information 5). For example, *E. coli* replicates its circular genome in a bidirectional manner from a single origin of replication. This simple mode of replication requires minimal clamp loading events to achieve continuous and uninterrupted leading and lagging strand DNA synthesis. In contrast, bacteriophage T4 DNA synthesis is more complicated as replication of its linear genome occurs in two distinct phase. After bidirectional DNA synthesis commences from fixed locations in the phage genome, there is a switch to recombination-dependent replication (RDR) that produces long concatemers of the phage genome generated via homologous recombination. RDR requires the activity of two additional bacteriophage enzymes, UvsX and UvsY, that utilize ATP to catalyze strand invasion of single stranded 3' ends of DNA into homologous regions of duplex DNA (D). After replication of the resulting 'D-loop' structures, the concatemers are processed into smaller genomic segments by terminase prior to packaging into new phage particles. Since efficient concatemeric replication depends upon a high frequency of clamp loading events, the bacteriophage is predicted to be more sensitive to the inhibitory effects of d5-NITP. In addition, d5-NITP could inhibit other targets associated with bacteriophage replication and/or infection including other ATP-dependent enzymes such as UvsX, UvsY, gp59 (DNA helicase), and gp 61 (helicase loader) that are required for RDR. Regardless, these data support a new approach to disrupt the activity of a specific replicative accessory protein in various DNA- and RNA-dependent viruses. This approach could be used to develop new therapeutic agents against herpes simplex virus (HSV) and hepatitis C virus whose life cycle



also depend on the activity of ATP-dependent accessory proteins (21). HSV is a particular relevant example since it possesses several accessory proteins, including the origin dependent replication initiator (UL9) and the DNA helicase-primase (UL5, UL52 core enzyme, and UL8 loader), that require ATP binding and hydrolysis for activity (22).

## Methods and Materials

### Materials

Non-natural nucleosides and nucleotides were synthesized as previously described (9, 23%<sub>000</sub>25). Purification of wild-type gp44/62 and gp45 from overproducing strains obtained from Dr. William Konigsberg (Yale University) was performed as previously described (26). The R175K and R175L mutants of gp44/62 were constructed and purified as described in Supplemental Table 1. Purification of exonuclease-deficient T4 DNA polymerase (D129A) was performed as previously described (27). The pET26b vector harboring the double mutant gp45 W199F V162C (28) was a generous gift from Dr. Stephen Benkovic (Pennsylvania State University). Expression, purification, and labeling of the mutant gp45 with 7-diethylamino-3-(4'-maleimidylphenyl)-4-methylcoumarin (CPM) (Molecular Probes) was done as described (28).

### Initial velocity studies in the presence and absence of inhibitor

All experiments with gp44/62 used the following buffer system (designated T4 buffer): 50 mM Tris pH 7.5, 10 mM DTT, 150 mM potassium acetate, 10% glycerol. A typical ATPase assay contained 10 mM Mg<sup>2+</sup>, 1 μM 13/20 DNA, 500 μM (r)NTP or (d)NTP, 500 nM gp45, and 500 nM gp44/62 in T4 buffer. ATPase activity was measured by monitoring the release of P<sub>i</sub> using a malachite green assay (29) or via the hydrolysis of [γ-<sup>32</sup>P]-ATP. Reaction inhibition studies used identical conditions except for the inclusion of variable concentrations of inhibitor (0–400 μM) and a fixed concentration of ATP (32.5 nM [γ-<sup>32</sup>P]-ATP and 100 μM unlabeled ATP). Reactions were quenched at variable times (0–120 seconds) by the addition of an equal volume of 1 N formic acid and analyzed by TLC on PEI-cellulose plates (EM Science) using 0.6 M KH<sub>2</sub>PO<sub>4</sub>, pH 3.5. The ATPase activity of the γ-complex was measured as above using the following modifications: all reactions were performed at 37°C, γ-complex buffer (20 mM Tris pH 7.5, 5 mM DTT, 10% glycerol) was used, the concentration of ATP was fixed at 20 μM, and 100 nM of β-subunit and γ-complex was used. Reactions were quenched using 0.5 M EDTA. In both cases, product formation was detected using a Packard Cyclone PhosphorImager. The ratio of free <sup>32</sup>P<sub>i</sub> to non-hydrolyzed [γ-<sup>32</sup>P]-ATP was multiplied by the final concentration of ATP to obtain total product concentration. Product formation in the absence of enzyme was measured and subtracted from all measurements. Initial velocities were obtained by fitting the data to equation 1.

$$y=mx+b \quad (1)$$

Y is product concentration, x is time, m is the slope, and b is the y-intercept. IC<sub>50</sub> values were obtained by fitting initial velocities to equation 2.

$$y=100/(1+(IC_{50}/I)^n) \quad (2)$$

y = fractional activity, I is the concentration of inhibitor, IC<sub>50</sub> is the concentration of inhibitor that yields 50% enzyme activity, and n is the Hill coefficient for the inhibitor. True Inhibition constants designated as K<sub>i</sub> values were obtained from equation 3:

$$K_i = IC_{50} / (1 + [ATP] / K_m) \quad (3)$$

$K_m$  is the Michaelis-Menten constant for ATP,  $[ATP]$  is the concentration of ATP, and  $IC_{50}$  the concentration of inhibitor that yields 50% enzyme activity.

### Replicase Formation Assay

34/Bio-62 (50SP)/36-mer was prepared and labeled as previously described (30). T4 buffer was mixed with 34/Bio-62 (50SP)/36-mer (500 nM), ATP (100  $\mu$ M),  $Mg^{2+}$  (10 mM), streptavidin (1  $\mu$ M), dCTP (500  $\mu$ M), gp44/62 (500 nM), gp45 (500 nM), and gp43  $exo^-$  (150 nM). Reaction was initiated with gp43  $exo^-$  and incubated for 10 seconds. Elongation was initiated by addition of (d)NTPs (100  $\mu$ M) with salmon sperm DNA trap (3 mg/ml) and quenched in an equal volume of 1 M HCl at variable time (0–15 seconds). DNA was extracted using phenol: chloroform: isoamyl alcohol (25:24:1) and neutralized with 1 M Tris/NaOH. Strands were separated on a 16% denaturing acrylamide gel and detected by phosphorimaging. The presence of full-length product (50-mer) is indicative of replicase formation.

### Fluorescence measurements

Tryptophan fluorescence was measured with a Kintek SF-2004 stopped-flow. Excitation wavelength was 290 nm and emission cutoff filter was 310 nm. Syringe A contained T4 buffer, 2  $\mu$ M gp44/62 and 20 mM  $Mg^{2+}$ . Syringe B contained T4 buffer, 2  $\mu$ M 45 W199F V162C-CPM, and 1 mM ATP or 1 mM d5-NITP. Single mixing reactions were monitored over 3 seconds and data were fit to the equation for a single exponential (Equation 4).

$$Y = A(1 - e^{-kt}) \quad (4)$$

A is the amplitude, k is the first-order rate constant, and t is time.

### *In vivo* Phage assay and toxicity screen

Initial screening of potential toxicity against *E. coli* was performed growing JA300 *E. coli* cells (ATCC) in the absence and presence of various non-natural nucleosides. The culture media was LB supplemented with 0.8 g glucose/liter. A 1:250 dilution of an overnight culture was grown to mid-log phase and treated with non-natural nucleoside for one hour. Growth curves were obtained by measuring  $OD_{600}$  and toxicity was assessed by comparing growth curves of cells treated with non-natural nucleosides and DMSO. Toxicity over a 24-hour period was assessed by plating dilutions of suspension cultures on LB/agar plates and counting colonies after 24 hours.

The inhibitory effects of various non-natural nucleosides against phage proliferation was assessed using a plaque forming assay. An overnight culture of JA300 *E. coli* cells was diluted 1:150 in LB and pre-incubated with varying concentrations of non-natural nucleosides for 60 minutes at 37°C. Cultures were then infected with ~300 pfu of T4 bacteriophage (ATCC). The suspension was decanted over an LB/agar plate. After the suspension absorbed into the LB/agar, plates were incubated at 37°C for 24 hours and plaques were manually counted. To test the dependence of non-natural nucleoside metabolism on phage inhibition, a deoxythymidine kinase knock out *E. coli* strain (KY895) (31, 32) was obtained from the *E. coli* Genetic Resource Center (Yale University) and used in place of JA300 in the plaque forming assay. In all cases, ANOVA analysis and student's t-test were performed using Graphpad Prism v4.0.

## Molecular modeling

An energy minimized coordinates of d5-NITP was generated from the Dundee PRODRG2 Server (<http://davapc1.bioch.dundee.ac.uk/programs/prodrg/>) (33). The structure of  $\gamma$ -complex used for modeling was obtained from the RCSB Protein Data Bank (PDBID: 1N9F). A model of gp44/62 was obtained by threading the primary sequence of gp44/62 was into the structure of *P. furiosus* RFC (24% sequence identity PDBID: 1IPQ) using the Imperial College Protein Homology/analogy Recognition Engine (PHYRE) (<http://www.sbg.bio.ic.ac.uk/phyre/>). d5-NITP was docked into the active site of each structure using Crystallographic Object-Oriented Toolkit (34). Docked models were then subject to energy minimization using CNSolve v. 1.1.

## Supplementary Material

Refer to Web version on PubMed Central for supplementary material.

## Acknowledgments

This research was supported through funding from the National Institutes of Health to AJB (CA118408) and from the National Institutes of Health to MDS (GM066094).

## References

1. Gerson SL. Clinical relevance of MGMT in the treatment of cancer. *J Clin Oncol.* 2002; 20(9): 2388–2399. [PubMed: 11981013]
2. David Golan, ATJ.; Ehrin, Armstrong; Joshua, Galanter; April, Armstrong; Ramy, Arnaout; Harris, Rose. *Principles of Pharmacology: The Pathophysiologic Basis of Drug Therapy.* Philadelphia: Lippincott Williams & Wilkens; 2005.
3. Laghi L, Bianchi P, Malesci A. Differences and evolution of the methods for the assessment of microsatellite instability. *Oncogene.* 2008; 27(49):6313–6321. [PubMed: 18679418]
4. Vigouroux C, Gharakhanian S, Salhi Y, Nguyen TH, Adda N, Rozenbaum W, Capeau J. Adverse metabolic disorders during highly active antiretroviral treatments (HAART) of HIV disease. *Diabetes Metab.* 1999; 25(5):383–392. [PubMed: 10592860]
5. Allan JM, Travis LB. Mechanisms of therapy-related carcinogenesis. *Nat Rev Cancer.* 2005; 5(12): 943–955. [PubMed: 16294218]
6. Johnson A, O'Donnell M. Cellular DNA replicases: components and dynamics at the replication fork. *Annu Rev Biochem.* 2005; 74:283–315. [PubMed: 15952889]
7. Mace DC, Alberts BM. The complex of T4 bacteriophage gene 44 and 62 replication proteins forms an ATPase that is stimulated by DNA and by T4 gene 45 protein. *J Mol Biol.* 1984; 177(2):279–293. [PubMed: 6235378]
8. Fradkin LG, Kornberg A. Prereplicative complexes of components of DNA polymerase III holoenzyme of *Escherichia coli*. *J Biol Chem.* 1992; 267(15):10318–10322. [PubMed: 1587819]
9. Zhang X, Lee I, Berdis AJ. Evaluating the contributions of desolvation and base-stacking during translesion DNA synthesis. *Org Biomol Chem.* 2004; 2(12):1703–1711. [PubMed: 15188037]
10. Mace DC, Alberts BM. Characterization of the stimulatory effect of T4 gene 45 protein and the gene 44/62 protein complex on DNA synthesis by T4 DNA polymerase. *J Mol Biol.* 1984; 177(2): 313–327. [PubMed: 6611423]
11. Copeland, R. *Evaluation of Enzyme Inhibitors in Drug Discovery: A Guide for Medicinal Chemists and Pharmacologists.* 1st ed.. New York: Wiley-Interscience; 2005.
12. Berdis AJ, Benkovic SJ. Mechanism of bacteriophage T4 DNA holoenzyme assembly: the 44/62 protein acts as a molecular motor. *Biochemistry.* 1997; 36(10):2733–2743. [PubMed: 9062100]
13. Kaboord BF, Benkovic SJ. Dual role of the 44/62 protein as a matchmaker protein and DNA polymerase chaperone during assembly of the bacteriophage T4 holoenzyme complex. *Biochemistry.* 1996; 35(3):1084–1092. [PubMed: 8547244]

14. Reineks EZ, Berdis AJ. Evaluating the effects of enhanced processivity and metal ions on translesion DNA replication catalyzed by the bacteriophage T4 DNA polymerase. *J Mol Biol.* 2003; 328(5):1027–1045. [PubMed: 12729739]
15. Reineks EZ, Berdis AJ. Evaluating the contribution of base stacking during translesion DNA replication. *Biochemistry.* 2004; 43(2):393–404. [PubMed: 14717593]
16. Kincaid K, Beckman J, Zivkovic A, Halcomb RL, Engels JW, Kuchta RD. Exploration of factors driving incorporation of unnatural dNTPS into DNA by Klenow fragment (DNA polymerase I) and DNA polymerase alpha. *Nucleic Acids Res.* 2005; 33(8):2620–2628. [PubMed: 15879351]
17. Alley SC, Abel-Santos E, Benkovic SJ. Tracking sliding clamp opening and closing during bacteriophage T4 DNA polymerase holoenzyme assembly. *Biochemistry.* 2000; 39(11):3076–3090. [PubMed: 10715129]
18. Kelley LA, Sternberg MJ. Protein structure prediction on the Web: a case study using the Phyre server. *Nat Protoc.* 2009; 4(3):363–371. [PubMed: 19247286]
19. Davey MJ, Jeruzalmi D, Kuriyan J, O'Donnell M. Motors and switches: AAA+ machines within the replisome. *Nat Rev Mol Cell Biol.* 2002; 3(11):826–835. [PubMed: 12415300]
20. Jim, D.; Karam, JWD. *Molecular biology of bacteriophage T4.* illustrated ed.. Washington DC: American Society for Microbiology; 1994.
21. Frick DN. The hepatitis C virus NS3 protein: a model RNA helicase and potential drug target. *Curr Issues Mol Biol.* 2007; 9(1):1–20. [PubMed: 17263143]
22. Nimonkar AV, Boehmer PE. Reconstitution of recombination-dependent DNA synthesis in herpes simplex virus 1. *Proc Natl Acad Sci U S A.* 2003; 100(18):10201–10206. [PubMed: 12928502]
23. Zhang X, Lee I, Berdis AJ. A potential chemotherapeutic strategy for the selective inhibition of promutagenic DNA synthesis by nonnatural nucleotides. *Biochemistry.* 2005; 44(39):13111–13121. [PubMed: 16185079]
24. Zhang X, Lee I, Berdis AJ. The use of nonnatural nucleotides to probe the contributions of shape complementarity and pi-electron surface area during DNA polymerization. *Biochemistry.* 2005; 44(39):13101–131010. [PubMed: 16185078]
25. Zhang X, Lee I, Zhou X, Berdis AJ. Hydrophobicity, shape, and pi-electron contributions during translesion DNA synthesis. *J Am Chem Soc.* 2006; 128(1):143–149. [PubMed: 16390141]
26. Morris CF, Hama-Inaba H, Mace D, Sinha NK, Alberts B. Purification of the gene 43, 44, 45, and 62 proteins of the bacteriophage T4 DNA replication apparatus. *J Biol Chem.* 1979; 254(14):6787–6796. [PubMed: 376534]
27. Frey MW, Nossal NG, Capson TL, Benkovic SJ. Construction and characterization of a bacteriophage T4 DNA polymerase deficient in 3'→5' exonuclease activity. *Proc Natl Acad Sci U S A.* 1993; 90(7):2579–2583. [PubMed: 8464864]
28. Alley SC, Shier VK, Abel-Santos E, Sexton DJ, Soumilion P, Benkovic SJ. Sliding clamp of the bacteriophage T4 polymerase has open and closed subunit interfaces in solution. *Biochemistry.* 1999; 38(24):7696–7709. [PubMed: 10387009]
29. Shirasaka Y, Onishi Y, Sakurai A, Nakagawa H, Ishikawa T, Yamashita S. Evaluation of human P-glycoprotein (MDR1/ABCB1) ATPase activity assay method by comparing with in vitro transport measurements: Michaelis-Menten kinetic analysis to estimate the affinity of P-glycoprotein to drugs. *Biol Pharm Bull.* 2006; 29(12):2465–2471. [PubMed: 17142983]
30. Kaboord BF, Benkovic SJ. Accessory proteins function as matchmakers in the assembly of the T4 DNA polymerase holoenzyme. *Curr Biol.* 1995; 5(2):149–157. [PubMed: 7743178]
31. Hiraga S, Igarashi K, Yura T. A deoxythymidine kinase-deficient mutant of *Escherichia coli*. I. Isolation and some properties. *Biochim Biophys Acta.* 1967; 145(1):41–51. [PubMed: 4228236]
32. Igarashi K, Hiraga S, Yura T. A deoxythymidine kinase deficient mutant of *Escherichia coli*. II. Mapping and transduction studies with phage phi 80. *Genetics.* 1967; 57(3):643–654. [PubMed: 4868676]
33. Schuttelkopf AW, van Aalten DM. PRODRG: a tool for high-throughput crystallography of protein-ligand complexes. *Acta Crystallogr D Biol Crystallogr.* 2004; 60(Pt 8):1355–1363. [PubMed: 15272157]
34. Emsley P, Cowtan K. Coot: model-building tools for molecular graphics. *Acta Crystallogr D Biol Crystallogr.* 2004; 60(Pt 12 Pt 1):2126–2132. [PubMed: 15572765]

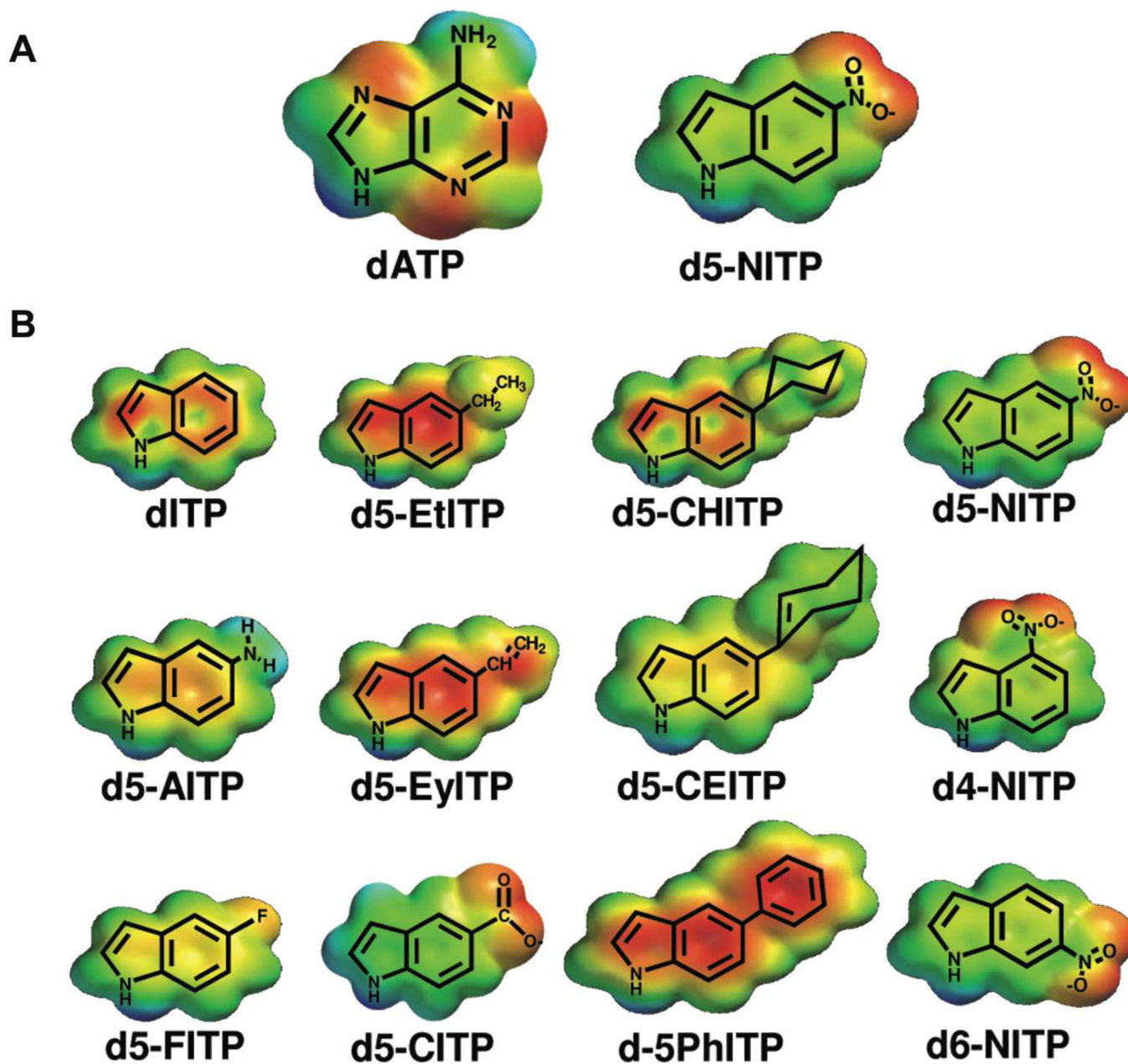


**Figure 1.** Structures and electron density surface potentials of natural and non-natural nucleosides and nucleotides used in this study. For convenience, only the nucleobase portion is provided. (A) Comparison of the structures of adenine and 5-nitroindole (B) Structures of substituted indolyl deoxynucleotides. All models were constructed using Spartan '04 software ([www.wavefun.com](http://www.wavefun.com)). The electron density surface potentials of adenine and non-natural nucleobases were then generated. The most electronegative regions are in red, neutral charges are in green, and the most electropositive regions are in blue.

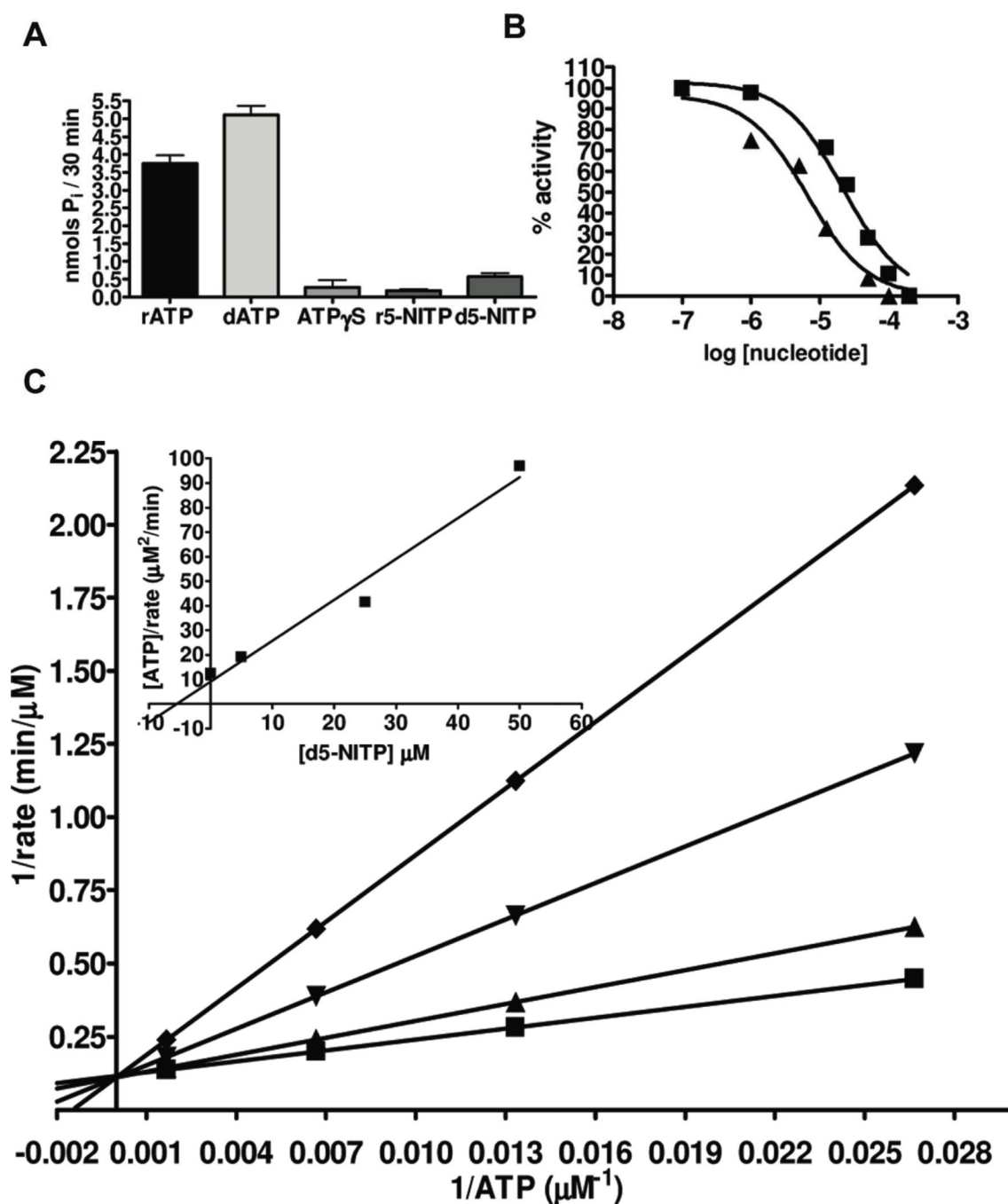


**Figure 2.** d5-NITP is not hydrolyzed by gp44/62 but instead acts as a competitive inhibitor. (A) Hydrolysis of various nucleotide substrates by gp44/62 quantified by colorimetric ATPase assay. Assay conditions are as described in methods section. The concentration of all nucleotide substrates was maintained at 500 μM (b) Dose-dependent inhibition of gp44/62 ATPase activity by d5-NITP (▲) and r5-NITP (■).  $K_i$  values are  $4.8 \pm 0.5$  μM and  $10.8 \pm 0.7$  μM, respectively. (c) Double reciprocal plot of rate versus ATP concentration at several fixed concentrations of d5-NITP. The following concentrations of d5-NITP were used: no inhibitor (■), 5 μM (▲), 25 μM (▼), and 50 μM (◆). The  $K_i$  value of d5-NITP was determined by fitting the data to the following rate equation:  $v = V_{\max}[S]/K_m(1+[I]/K_i) +$

[S]. The inset shows a plot of the slope of each line ( $[ATP]/rate$ ) as a function of d5-NITP concentration.

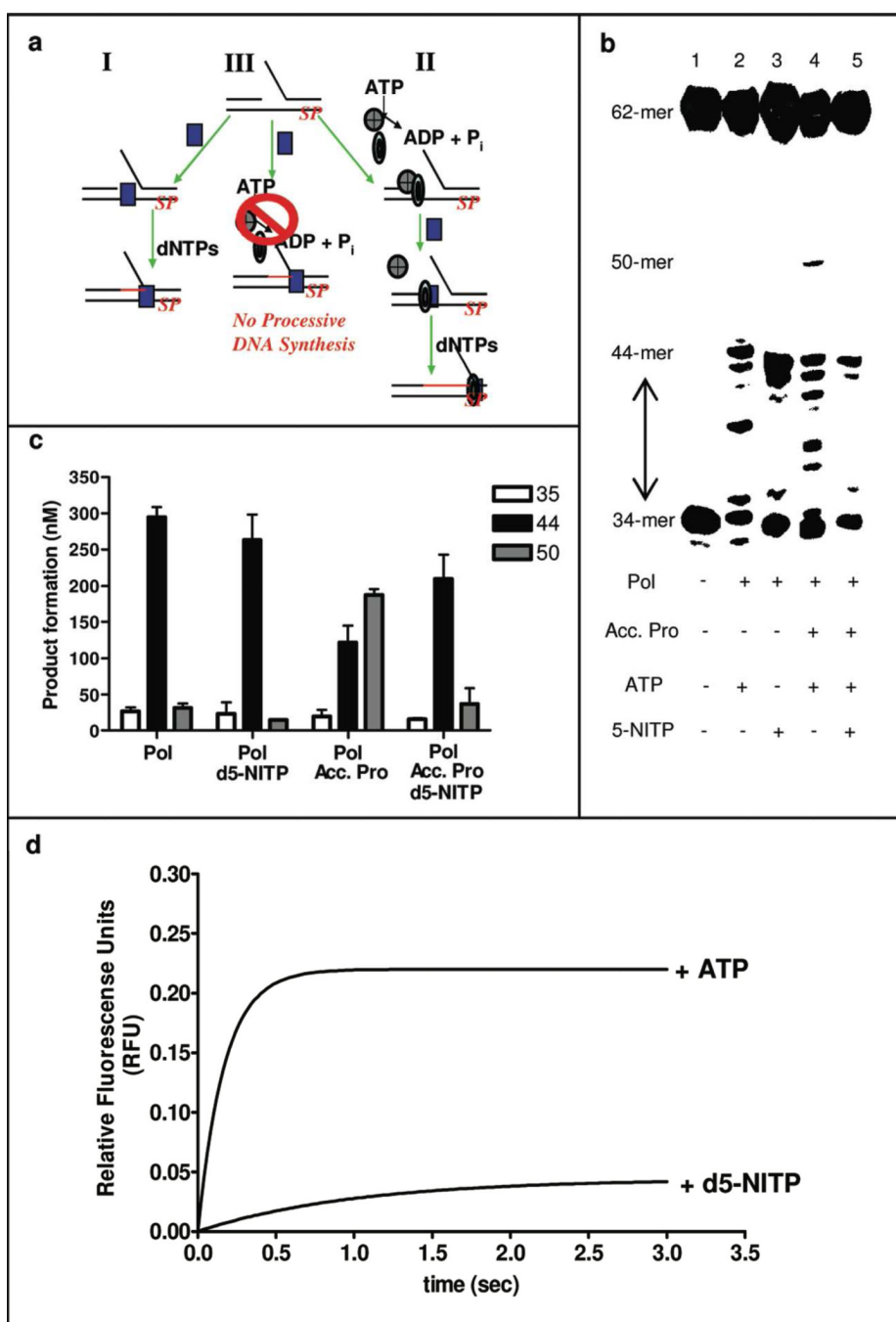


**Figure 3.** d5-NITP inhibits assembly of the bacteriophage T4 replicase. (A) Diagram of strand displacement assay used to monitor replicase assembly and function. DNA polymerase alone (I) can incorporate nucleotides up to the forked strand but is unable to extend beyond it. As such, the longest product possible is a 44-mer. DNA polymerase in the presence of accessory proteins (II) defines the replicase and is able to extend the primer beyond the forked strand up to the abasic site (SP) present at position 51 in the template. In this case, the longest product formed is a 50-mer. When an ATPase inhibitor is present (III), replicase assembly is prevented. As a result, extension beyond the forked strand is not observed and the longest product detected is 44-mer generated by DNA polymerase alone. (b)



Representative denaturing gel electrophoretic images of DNA synthesis catalyzed by the bacteriophage T4 polymerase and replicase in the absence or presence of d5-NITP. DNA substrate alone (lane 1), T4 DNA polymerase (lane 2), T4 DNA replicase (polymerase and accessory proteins) (lane 4), T4 DNA polymerase with 100  $\mu$ M d5-NITP (lane 3), and T4 DNA replicase with 100  $\mu$ M d5-NITP. (lane 5) (C) Quantification of product formation using the strand displacement assay described above. (D) Fluorescence changes associated with opening of the bacteriophage T4 processivity factor by the clamp loader, gp44/62. In the presence of 1 mM ATP, gp44/62 opens the closed ring of the homotrimeric gp45 labeled with fluorescent probe to generate a rapid change in fluorescence. In the presence of 1 mM d5-NITP, a significantly smaller change in fluorescence is observed indicating that clamp opening does not occur upon binding of the non-natural nucleotide.

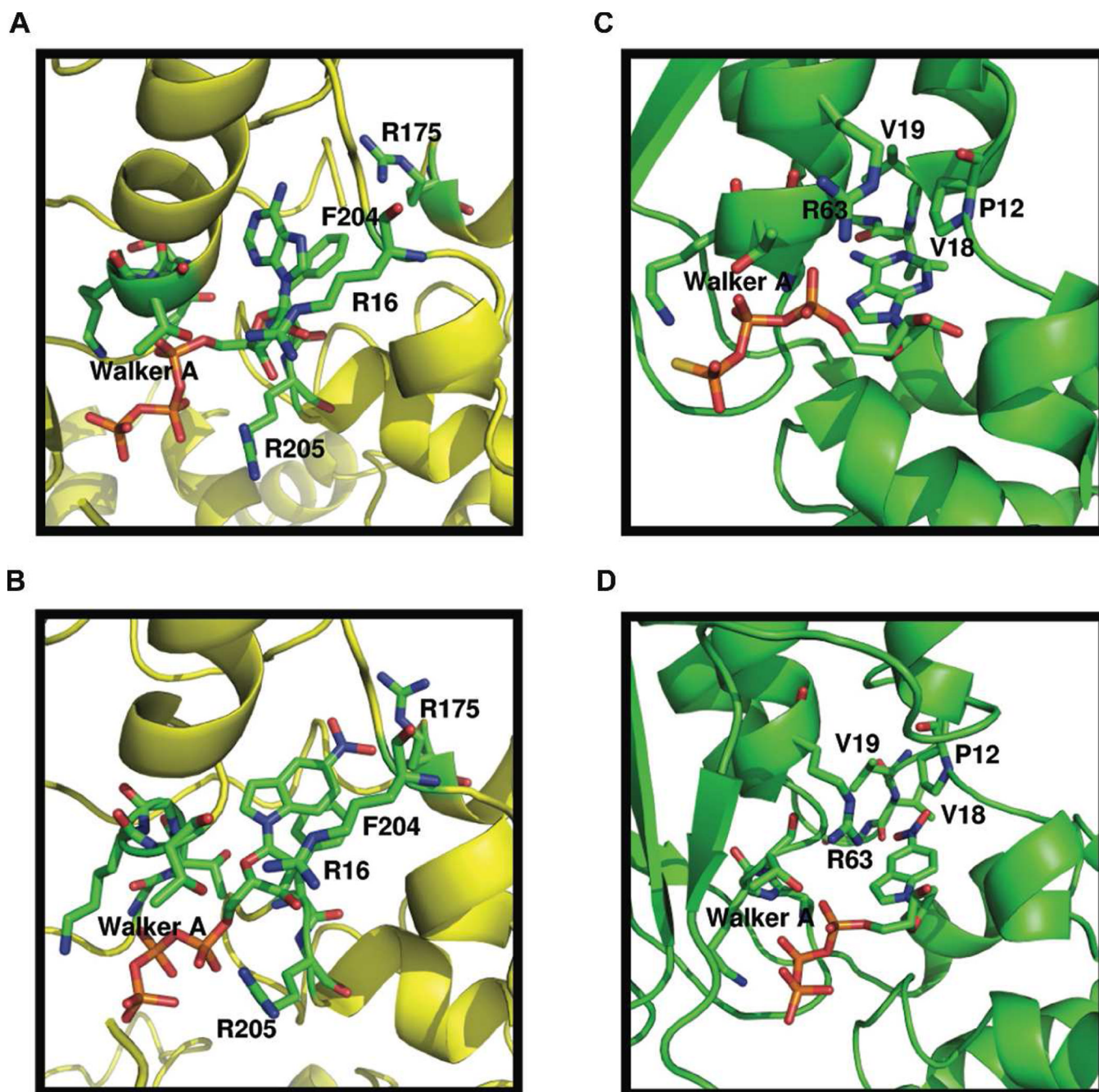


**Figure 4.** Molecular modeling of the active sites of gp44/62 and  $\gamma$ -complex. The active site of the bacteriophage T4 clamp loader, gp44/62, bound with (A) ATP or (B) d5-NITP. The active site of the *E. coli* clamp loader,  $\gamma$ -complex, bound with (C) ATP or (D) d5-NITP.

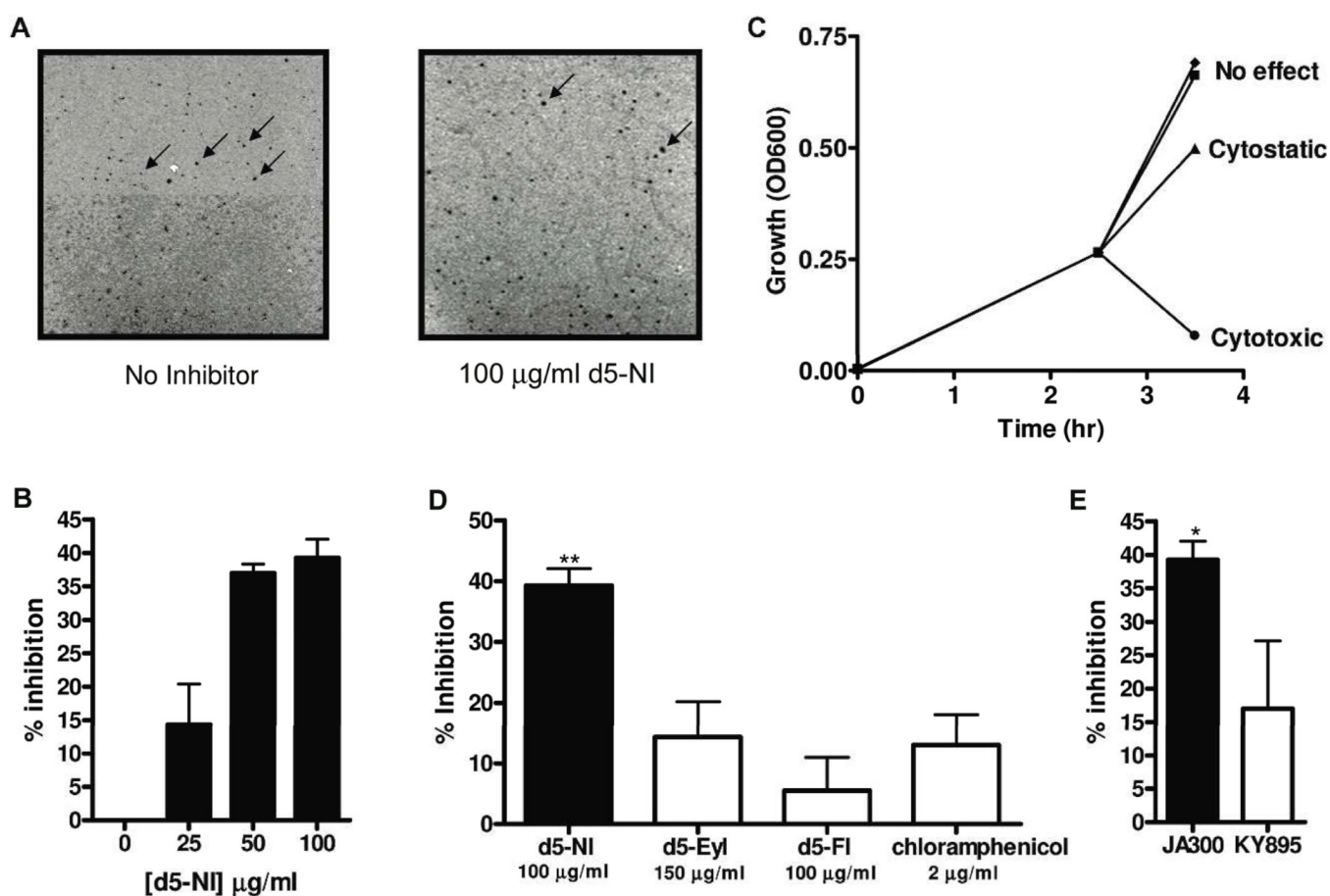


**Figure 5.** Inhibition of T4 plaque formation by d5-NI. (A) The addition of 100 µg/ml d5-NI reduces plaque formation. Arrows indicate plaques caused by the lysis of phage-infected *E. coli*. (B) Graphical quantification of plaque reduction by d5-NI (n=4, \*\*p<0.01 vs others). (C) Effects of 100 µg/ml d5-NI (◆), d5-EyI (▲) and ampicillin (●) compared to a DMSO control treated normal growth curve of *E. coli* (■). (D) Comparing the ability of d5-NI, d5-EyI, d5-FI, and chloramphenicol to inhibit phage infectivity. (n=4, \*\*p<0.01 vs others) (E) The addition of 100 µg/ml d5-NI reduces plaque formation more effectively in wild type *E. coli* (JA300) compared to the *E. coli* strain, KY895, that is deficient in deoxythymidine kinase activity (*tdk-1*). (n=3, \*p<0.05).

**Table 1**

Summary of inhibition constants for natural and non-natural nucleotides against the ATP-dependent clamp loaders from bacteriophage T4 (gp44/62) and *Escherichia coli* ( $\gamma$ -complex).

Nucleotide Analog	gp44/62 K <sub>i</sub> ( $\mu$ M) <sup>a</sup>	$\gamma$ -complex K <sub>i</sub> ( $\mu$ M) <sup>b</sup>	Selectivity Factor <sup>c</sup>
ATP $\gamma$ S	28.9 $\pm$ 11.6	13.0 $\pm$ 4.5	0.44
dITP	<200 <sup>d</sup>	60.9 $\pm$ 19.5	0.30
d5-AITP	<200	45.0 $\pm$ 18.5	0.23
d5-FITP	<200	34 $\pm$ 4	0.17
d5-EtITP	81.5 $\pm$ 17.0	9.0 $\pm$ 3.2	0.11
d5-EyITP	<200	30.0 $\pm$ 15.7	0.15
d5-CITP	37 $\pm$ 8	40 $\pm$ 13	0.93
d5-NITP	4.8 $\pm$ 0.5	21.7 $\pm$ 2.1	4.52
d5-CHITP	47.5 $\pm$ 10.0	24.0 $\pm$ 10.5	0.51
d5-CEITP	10.0 $\pm$ 1.6	11.8 $\pm$ 1.5	1.18
d5-PhITP	42 $\pm$ 10	7.5 $\pm$ 1.1	0.18
d4-NITP	34.2 $\pm$ 6.7	11.1 $\pm$ 2.4	0.32
d6-NITP	5.1 $\pm$ 1.4	8.1 $\pm$ 2.3	1.59

<sup>a</sup> Reactions were performed using 500 nM gp44/62 and gp45, 10 mM Mg<sup>2+</sup>, 100  $\mu$ M ATP, 1  $\mu$ M DNA. The concentration of nucleotide was varied from 0.5–400  $\mu$ M. Assays were performed at 25°C. Initial rates in ATP consumption were obtained from the time courses that were linear over the time frame measured (120 seconds). IC<sub>50</sub> values were converted to dissociation constants (K<sub>i</sub>) using equation 3.

<sup>b</sup> Reactions were performed using 100 nM  $\gamma$ -complex and  $\beta$ -clamp, 10 mM Mg<sup>2+</sup>, 20  $\mu$ M ATP, 1  $\mu$ M DNA. The concentration of nucleotide was varied from 0.5–400  $\mu$ M. Assay was performed at 37°C. Initial rates in ATP consumption were obtained from the time courses that were linear over the time frame measured (120 seconds). IC<sub>50</sub> values were converted to dissociation constants (K<sub>i</sub>) using equation 3.

<sup>c</sup> Selectivity Factor = K<sub>i</sub> ( $\gamma$ -complex) / K<sub>i</sub> (gp44/62).

<sup>d</sup> No inhibition was observed at nucleotide concentrations greater than 200  $\mu$ M.

**Table 2**

Summary of inhibition constants for various non-natural nucleotides against wild-type, R175K, and R175L mutants of gp44/62.

Nucleotide Analog	Wild-type $K_i$ ( $\mu\text{M}$ ) <sup>a</sup>	R175K $K_i$ ( $\mu\text{M}$ )	R175L $K_i$ ( $\mu\text{M}$ )
ATP $\gamma$ S	28.9 $\pm$ 11.6	14.0 $\pm$ 3.5	33.2 $\pm$ 8.0
d5-NITP	4.8 $\pm$ 0.5	13.8 $\pm$ 4.2	16.4 $\pm$ 2.4
d5-CITP	37 $\pm$ 8	40.6 $\pm$ 17.6	<200 <sup>b</sup>
d5-EtITP	81.5 $\pm$ 17.0	25.2 $\pm$ 4.2	11.0 $\pm$ 3.5
d5-EyITP	<200	26.2 $\pm$ 9.0	34 $\pm$ 14
d4-NITP	34.2 $\pm$ 6.7	30.2 $\pm$ 7.4	41.6 $\pm$ 10.9
d6-NITP	5.1 $\pm$ 1.4	9.1 $\pm$ 2.1	5.0 $\pm$ 1.8

<sup>a</sup> Reactions were performed using 500 nM gp44/62 and gp45, 10 mM Mg<sup>2+</sup>, 100  $\mu\text{M}$  ATP, 1  $\mu\text{M}$  DNA. The concentration of nucleotide was varied from 0.5–400  $\mu\text{M}$ . Assays were performed at 25°C. Initial rates in ATP consumption were obtained from the time courses that were linear over the time frame measured (120 seconds). IC<sub>50</sub> values were converted to dissociation constants ( $K_i$ ) using equation 3.

<sup>b</sup> No inhibition was observed at nucleotide concentrations greater than 200  $\mu\text{M}$ .